2

institut de physique nucléaire
LABORATOIRE ASSOCIÉ A L'IN2P3

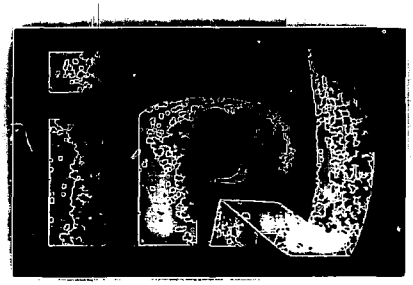

IPNO DRE 83-30

THE COMPLEX TRANSFER REACTION (^{14}C, ^{15}C) ON Ni, Zn AND Ge TARGETS ; EXISTENCE AND MASS OF ^{69}Ni

Ph.Dessagne, M.Bernas, M.Langevin, C.Morrison, J.Payet

F.Pougheon and P.Roussel

UNIVERSITÉ PARIS SUD

IPNO DRE 83-30

THE COMPLEX TRANSFER REACTION (^{14}C, ^{15}O) ON Ni,Zn AND Ge TARGETS ; EXISTENCE AND MASS OF ^{69}Ni

Ph.Dessagne, M.Bernas, M.Langevin, G.Morrison, J.Payet

F.Pougheon and P.Roussel

THE COMPLEX TRANSFER REACTION (^{14}C, ^{15}O) ON Ni, Zn AND Ge TARGETS ; EXISTENCE AND MASS OF ^{69}Ni

PH. DESSAGNE(x), M. BERNAS, M. LANGEVIN, G.C. MORRISSON(*),
J. PAYET, F. POUGHEON, P. ROUSSEL

Institut de Physique Nucléaire d'Orsay
B.P. N°1, 91406 Orsay

Abstract : The (^{14}C, ^{15}O) complex transfer reaction has been studied at 72 Mev incident energy on $^{58,60,62,64}Ni$, $^{68,70}Zn$ and $^{74,76}Ge$ targets. Spectra and differential cross sections have been measured in a 5° angular range centred around a laboratory angle of 6°. The nucleus ^{69}Ni has been observed and its mass determined for the first time.

NUCLEAR REACTIONS : $^{58,60,62,64}Ni(^{14}C, ^{15}O)$ $^{57,59,61,63}Fe$, $^{68,70}Zn(^{14}C, ^{15}O)^{67,69}Ni$ and $^{74,76}Ge(^{14}C, ^{15}O)^{73,75}Zn$, E = 72 Mev. Measured spectra, reaction cross sections, and ^{69}Ni mass excess.

(x) Present adress; Centre de Recherches Nucleaires B.P. 20 Strasbourg Cedex 67037 FRANCE

(*) Permanent address : University of Birmingham, Department of Physics, P.O. Box 363 - Birmingham, ENGLAND.

1. INTRODUCTION

The (^{14}C,^{15}O) complex transfer reaction combines the pick-up of two charges with that of only one mass unit. When performed on the neutron-rich ridge of the stability valley it leads to nuclei further away from this valley.

Even isotopes of Ni, Zn and Ge were chosen as target nuclei. For the heavier isotopes, the even odd nuclei populated by this transfer, namely ^{63}Fe, ^{69}Ni and ^{75}Zn are unknown, since they are not produced with large enough yield by fission and they are not yet studied by spallation and fragmentation reactions. Besides, this choice of target nuclei allows an extended investigation of the Z = 28 region.

The (^{14}C,^{15}O) reaction has only been reported once on a ^{40}Ca target[1]. The cross sections were measured to be one order of magnitude smaller than for the (^{14}C,^{16}O) reaction on the same target nuclei. From the (^{14}C,^{16}O) reaction already studied on the series of even Ni and Zn isotopes, reaction cross-sections of some 10μb/sr could be reasonably expected here.

2. EXPERIMENT

a) Set-up

The 72 MeV ^{14}C beam of 20 particle-nA was provided by the Orsay MP tandem. Except for ^{64}Ni and ^{70}Zn, the targets were prepared by evaporation of isotopes, enriched to better than 95%, with thicknesses ranging from 120 to 250μg/cm^2. For ^{64}Ni and ^{70}Zn it was found necessary to improve the isotopic purity and the mass separator "Paris" of the R. Bernas Laboratory was used for both isotopes.

In this way a 270 μg/cm^2 self supported ^{64}Ni target and a 80 μg/cm^2 ^{70}Zn target on a ^{12}C backing were prepared with an enrichment better than 99%.

The ^{15}O ions were analysed in a double-focusing n=1/2 magnetic spectometer. Two position-sensitive proportional counters spaced 40cm apart in the focal space provided the ion trajectories. The ion identification was achieved in a ΔE_1-ΔE_2-E ionization chamber; the vertical coordinate of each trajectory was also derived from the charge drift-time. The magnetic rigidity Bρ and the reaction angle were calculated on line [3] for each ion. The angular accuracy is 0.3° within a total angular aperture of 5°. An energy resolution of 120 keV was achieved for the thinner target of ^{70}Zn.

All the measurements were performed at θ_{lab}=6°(±2.5°).

b) Back-ground and calibration

The ΔE-E plot of the events observed in the focal plane is reported on fig.1.From there,and using double identification when necessary,the ^{15}O selection was achieved unambiguously.The spectra,calculated in term of magnetic rigidity corrected for kinemetical effects are shown on fig.2 to 4 and on fig.9 and fig.10.

The back-ground yield,which can be evaluated from that part of the spectra corresponding to "negative" excitation energies,remains at a level of ∿1 μb/sr.

As mentionned before,because of a careful multi parametric analysis of the data,there is no doubt on the ^{15}O identification for each selected event. Moreover impurities in the beam are less than 1 in 10^6 and usually much less. Hence the observed background has to be attributed to target contaminants both isotopic (all cases) and chemical (for the case of the mass separated ^{64}Ni and ^{70}Zn targets).

For the magnetic field corresponding to the ^{15}O of interest in the spectrometer,there is only one peak from an other two body reaction which could be recorded with a significant counting rate,namely a peak of ^{15}O from the (^{14}C,^{15}O) reaction on the oxygen contaminant of the ^{70}Zn target.

Therefore the calibration curves had to include data of ^{16}O-^{17}O associated to a higher magnetic field and this procedure contributes mainly to the error bars listed on the table 1.A test of consistency is provided by the mass-measurement of the same final nuclei from the two reactions A,Z (^{14}C,^{15}O) and A+2,Z (^{14}C,^{17}O) ref.4;it confirms the estimation of the errors.

3.RESULTS

a) Reaction mechanism,selectivity and spectroscopy

We first analyse the spectra from the (^{14}C,^{15}O) reaction on the serie of Ni isotopes in term of the number of neutron pairs (N/2) or of the reaction Q value , both being almost linearly dependant.On the energy spectra of ^{57}Fe and ^{59}Fe - corresponding to ^{58}Ni and ^{60}Ni targets,fig.2 and 3 - few levels are populated.For the more neutron rich nuclei,^{61}Fe and ^{63}Fe (fig.4) - corresponding to ^{62}Ni and ^{64}Ni targets - levels are more difficult to identify and the observation of g.s. becomes impossible for ^{63}Fe.

The reaction mechanism of ($^{14}C,^{15}O$) transfering two charges and only one mass unit can involve either the exchange of three particles ($^{14}C,^{16}O$)($^{16}O,^{15}O$) and ($^{14}C,^{13}C$)($^{13}C,^{15}O$) or the exchange of one particle combined with one charge exchange as ($^{14}C,^{14}N$)($^{14}N,^{15}O$) and ($^{14}C,^{15}N$)($^{15}N,^{15}O$). For incident energies of 5Mev/nucl the two particle transfer should be larger than the charge exchange process[5] and even more when the energy matching is appropriate for the former process. Thus the main route would be ($^{14}C,^{16}O$)($^{16}O,^{15}O$) as discussed in ref. 1. In another complex transfer $^{48}Ca(^{16}O,^{15}C)$ [6] the data were successfully reproduced with an exact finite range couple channel calculation, when the dominant route was ($^{16}O,^{14}C$)($^{14}C,^{15}C$) [7].

In this complex transfer, the ($^{14}C,^{16}O$) step was already measured [2]. It was shown to selectively populate the g.s. of the residual even-even Fe nuclei. Therefore, the spectra of even-odd Fe obtained here, should be related with the other step, namely ($^{16}O,^{15}O$), and it is worth to compare those spectra with the one resulting from a better known stripping reaction the (d,p) performed on stable even Fe targets as ^{56}Fe and ^{58}Fe.

On fig.2 and 3 are plotted schematically the spectra measured for (d,p) at deuteron energies of 5Mev/nucl (ref.8-9) and for the first maximum of angular distribution.

There is an obvious similarity between the ^{57}Fe spectra obtained with the two reactions which is no longer observed for ^{59}Fe. The spin values reported on fig.2 and 3 indicates the subshell on which the stripping occurs, namely $2p(1/2-)$, $2p(3/2-)$ and $1f(5/2-)$. No obvious l or j selectivity emerge from this comparison and the energy mismatch suffices to explain the small intensity of the 4.45Mev in ^{57}Fe and the dumping of low energy states in ^{59}Fe. Furthermore on spectra of heavier Fe residual nuclei, ^{61}Fe and ^{63}Fe (fig.4) only a group of excited states are populated while g.s. are not clearly observed.

The effect of the energy mismatch is more obvious on the ($^{14}C,^{15}O$) cross sections; reported on fig.5 as function of the reaction Q values, they are shown to decrease with one order of magnitude for $\Delta Q \simeq 3.5$Mev, i.e. for each extra-pair of neutrons.

It is interesting to compare once more with the one-neutron stripping reaction; the (d,p) transfer cross section decreases with a factor of almost 2 from ^{57}Fe to ^{59}Fe, as the 2p subshell offers almost twice less vacancies in the second case.

For ^{61}Fe, the g.s. with a spin value of $3/2^-$ [10] would be weakly populated as the 2p subshell should be filled up (in a crude shell model) in the intermediate ^{60}Fe nucleus. But ^{63}Fe, the g.s. of which was recently assigned to be $5/2^-$ [11] should be well populated given the emptyness of the $1f_{5/2}$ subshell.

Unfortunately at energies of 5Mev/n the Q effect is over passing those structure effects and the exponential fall of cross sections prevents from observing any of those two Fe g.s.

This strong Q effect is emphasized by the crossed exchange of nucleons in the (^{14}C,^{15}O) reaction. It can be seen by comparing with the (^{14}C,^{16}O) Q dependance of cross section[2] or with the (^{14}C,^{17}O) one (fig.6). Those last datas have been recorded simultaneously with (^{14}C,^{16}O) as ^{16}O and ^{17}O ejectiles occur with similar magnetic rigidity.

In both cases a smooth variation of cross sections is observed except for the ^{58}Ni target nuclei for which pick up cross sections are the smallest while the (^{14}C,^{15}O) cross section is the largest.

For the (^{14}C,^{16}O) reaction, the small Q dependance was accounted for within DWBA calculations[2] and the spectroscopic factors $S^2 \equiv d\sigma/d\Omega_{exp}/d\sigma/d\Omega_{DWBA}$ were qualitatively explained including deformations of initial and final nuclei and calculated in the frame of Hartree-Fock-Bogoliubov model[12].

The whole results are represented on a scheme (fig.7) crossing the stability valley, the average bottom of which goes by ^{56}Fe and approximately between ^{60}Ni and ^{61}Ni. This situation explains the sense of variation of the cross section on the neutron rich side.

However for (^{14}C,^{16}O) and even (^{14}C,^{17}O) reaction on the proton rich ^{58}Ni nuclei, the cross sections should be larger according to the direction of transfer optimizing the binding energy.

On the ^{68}Zn and ^{70}Zn target nuclei, the (^{14}C,^{15}O) reaction populates the g.s. of ^{67}Ni and ^{69}Ni which are clearly observed (fig.8). Larger by one order of magnitude (fig.5) those cross sections show the same Q value dependance as on Ni targets. It can be explained by the presence of two protons lying out of the $f_{7/2}$ closed shell, but the effect would take place as well for (^{14}C,^{16}O) or (^{14}C,^{17}O) while it reaches only a factor of two in both cases (fig.6).

Angular distributions were taken for the Zn targets (fig.9); they indicates a localisation of the process in the l-space by the occurence of a diffraction minimum at $\theta cm = 7°$.

For the ^{74}Ge and ^{76}Ge targets as well, larger cross sections are measured and on spectra (fig.10) the g.s. of ^{73}Zn and ^{75}Zn are observable even with shorter countings.

b) Mass measurement

Among the residual nuclei reached with (^{14}C, ^{15}O), some have never been observed before, as ^{69}Ni and ^{75}Zn. For ^{67}Ni, ^{73}Zn and ^{61}Fe the mass excesses were measured by (^{14}C, ^{17}O) and they are reported on the ^{15}O spectra (fig.4, 10 and 11) in order to check the consistency of the different calibrations. Mass excesses of ^{61}Fe and ^{67}Ni have been obtained also by (α, ^{7}Be) transfering two protons and one neutron, as in (^{14}C, ^{17}O)) but with a better energy resolution.

The mass excesses are listed and compared with previous results on the table. On fig.11, the two neutron binding energies are plotted as function of the number of mass A, in the region of study. This quantity is usually choosen in order to suppress the odd-even nuclei effect. The values for ^{74}Zn, ^{68}Ni and ^{62}Fe obtained from (^{14}C, ^{16}O) [2] and from the recent study of (^{18}O, ^{20}Ne) [13] are plotted also.

For ^{61}Fe (fig.4) the mass excess measured by ^{64}Ni (^{14}C, ^{17}O) [4] is compatible with the (^{14}C, ^{15}O) spectra. However the other determination, performed with ^{64}Ni (α, ^{7}Be) [14] differs with our result by 260 keV. We may indeed surestimate the ^{61}Fe mass, by mixing the ground state with the first excited state ≈360 keV [15] while they would be separated with (α, ^{7}Be) - where there is an indication for this level [14].

The first ^{67}Ni mass determination was resulting from a β-end point analysis [16] where the β analysed have been wrongly attributed to ^{67}Ni as shown in ref.11. The mass excess measured here with (^{14}C, ^{15}O) agrees with the value obtained with (^{14}C, ^{17}O) and with the result of (α, ^{7}Be) [17].

The ^{69}Ni nucleus is observed and its mass is measured here for the first time; the result obtained is compatible with an extrapolation of the Ni binding energies (fig.11).

The (^{14}C, ^{15}O) reaction on ^{74}Ge and ^{76}Ge targets leads to ^{73}Zn and ^{75}Zn final nuclei. The mass of ^{73}Zn was previously measured with the (^{14}C, ^{17}O) reaction and compared to the β-decay end-point extrapolation [18]. The result obtained here is less accurate but nevertheless agrees with this determination. The nucleus ^{75}Zn has not been previously observed, the (^{14}C, ^{15}O) spectrum shows indication for a mass value in agreement with the previous extrapolation [19].

On the table are also reported the mass excesses predicted by Liran-Zeldes and Janecke-Garvey-Kelson [20] and by Möller and Nix [21]. The measured mass-excess values lie between Liran-Zeldes and Janecke-Garvey-Kelson values, except for ^{67}Ni (for which both predictions are the same) and ^{69}Ni, the two nickel nuclei being more bound than calculated. The recent Möller and Nix calculation includes only few parameters but provides slightly too heavy nuclei.

4. CONCLUSION

A first systematic study of the (^{14}C,^{15}O) reaction at the incident of 72 Mev has been performed. The reaction mechanism has been analysed qualitatively, in term of (^{14}C,^{16}O),(^{16}O,^{15}O) and compared with (^{14}C,^{16}O) and (^{17}C,^{17}O) reactions previously measured on the same target nuclei.

At this energy the reaction shows a very strong Q (or neutron number) dependance which makes it difficult -low background level and long counting rate- to use for measuring exotic nuclei properties. Furthermore the g.s. of the final nuclei are weakly populated. However the ^{69}Ni nucleus has been unambiguously observed and its mass measured for the first time; indications on the production of ^{75}Zn and on its mass were also obtained.

We wish to aknowledge J.P. Mouffron for developping the ^{14}C ion source at the M.P. tandem, R.Meunier and the C.S.N.S.M. crew for preparing the ^{70}Zn and ^{64}Ni targets with the mass separator and Dr. G.Audi for usefull comments on binding energies of neutron rich nuclei.

REFERENCES

/1/ D.M. Drake, J.D. Moses, J.C. Peng, Nelson Stein and J.W. Sunier
Phys. Rev. Lett. 45 (1980) 1765

/2/ M. Bernas, J.C. Peng, H. Doubre, M. Langevin, M.J. Levine, F. Pougheon and P. Roussel
Phys. Rev. 24 (1981) 756

/3/ P. Roussel, M. Bernas, F. Diaf, F. Naulin, F. Pougheon, G. Ratbard and M. Roy-Stéphan
Nucl. Instr. and Meth. 153 (1978) 111

/4/ M. Bernas, Ph. Dessagne, M. Langevin, J. Payet, F. Pougheon, P. Roussel, I. Turkiewizc, M. Girod
To be published

/5/ D.R. Bes, O. Dragún and E.E. Maqueda
Nucl. Phys. A 405 (1983) 313

/6/ D.G. Kovar, W. Henning, E. Zeidman, Y. Eisen and H.T. Fortune
Phys. Rev. Lett. 33 (1974) 1611

/7/ T. Ugadawa, T. Tamura and K.S. Low
Phys. Rev. Lett. 34 (1975) 30

/8/ H.M. Sen gupta, A.R. Rajmunder and E.K. Liu
Nucl. Phys. A 160 (1971) 529

/9/ K.C. Mac Lean, S.M. Dagliesch, S.S. Ipson and G. Brown
Nucl. Phys. A 191 (1972) 417

/10/ C.M. Lederer and V.S. Shirley
Table of Isotopes, 7th edition (1978)

/11/ E. Runte, W.D. Schmidt-Ott, P. Tidemand-Peterson, R. Kirchner, O. Klepper, W. Kurcewizc, E. Roeckl, N. Kaffrell, P. Peuser, K. Rykaczewski, M. Bernas, Ph. Dessagne and M. Langevin
Nucl. Phys. A 399 (1978) 111

/12/ Ph. Dessagne and M. Girod Communication at the
International Conference on Nuclear Structure
Amsterdam 1982

/13/ R. Haupt, C.A. Wiedner, G.J. Wagner, K. Wannebo, T.S. Bathia, H. Haner, R. Mashuw, W. Saathoff and S.T. Thornton, submitted to Z. fur P.

/14/ J.D. Cossairt, R.E. Tribble and R.A. Kenefick
Phys. Rev. C 15 (1977) 1685

/15/ W.D. Schmidt-Ott, private communication

/16/ L.M. Taff, B.K.S. Koene and J. Van Klinken
Nucl. Phys. A 164 (1971) 565

/17/ R.T. Kouzes, D. Mueller and C. Yu
Phys. Rev. C 18 (1978) 1587

/18/ M. Bernas, Ph. Dessagne, M. Langevin, J. Payet, F. Pougheon, P. Roussel, W.D. Schmidt-Ott, P. Tidemand-Peterson and M. Girod
Accepted for publication in Nucl. Phys.

/19/ The 1977 atomic mass evaluation
A.H. Wapstra At. Nucl. Data Tables 19 (1977) 175

/20/ The 1975 Mass Predictions, ed. S. Maripuu
At. Nucl. Data Tables 17 (1976) 476

/21/ P. Möller and R. Nix
At. Nucl. Data Tables 16 (1981) 165

FIGURE CAPTION

Fig. 1 Bidimensional plot (ΔE-E) of ejectiles selected by the magnet at the ^{15}O magnetic rigidity Bρ.

Fig. 2 Energy spectrum of ^{15}O from the ^{58}Ni (^{14}C,^{15}O) ^{57}Fe reaction at 72 Mev. The differential cross sections of the (d,p) reaction on ^{56}Fe are plotted on the top part of the figure for comparison.

Fig. 3 Energy spectrum of ^{15}O from the ^{60}Ni (^{14}C,^{15}O)^{59}Fe reaction to compare with ^{58}Fe (d,p) cross sections as on fig.2.

Fig. 4 Energy spectra of the (^{14}C,^{15}O) reaction leading to ^{61}Fe and ^{63}Fe. They are displaced along the magnetic rigidity (Bρ) axis, so as to estimate the possible role of isotope contamination.

Fig. 5 The (^{14}C,^{15}O) cross section integrated upon 5°lab, versus the reaction Q value.

Fig. 6 Cross sections for the (^{14}C,^{16}O) - part a - and (^{14}C,^{17}O) - part b - reactions on series of even Ni and Zn isotopes.

Fig. 7 Relative cross sections for the pick-up of two protons (^{14}C,^{16}O), of two protons plus one neutron (^{14}C,^{17}O) and two protons minus one neutron (^{14}C,^{15}O) connecting even Ni nuclei with Fe g.s.

Fig. 8 Energy spectra of the (^{14}C,^{15}O) reaction leading to ^{67}Ni and ^{69}Ni nuclei, displaced so as to correspond to the same Bρ scale. The ^{69}Ni spectra results from the addition of two measurements performed with different magnetic fields.

Fig. 9 The typical angular distribution for the (^{14}C,^{15}O) reaction, measured between 5 and 10° c.m., shows an indication of diffraction minimum between 6 and 7°.

Fig. 10 Energy spectra of the (^{14}C,^{15}O) reaction leading to ^{73}Zn and ^{75}Zn, plotted on the same Bρ scale.

Fig. 11 Binding energies of two neutrons versus mass number A in the region of Ni, Zn. Crosses refer to previous results, circles to tabulated or extrapolated values and the points with error bars to our results. For ^{63}Fe, the dotted line correspond to the extrapolated value based on our ^{61}Fe mass value.

NUCLEI	MEASUREMENTS		PREDICTIONS		
	Previous results	This work	L.Z.[17]	J.G.K.[17]	M.N.[21]
^{61}Fe	- 59.01 ± 0.07 - 58.66 ± 0.10 (*) - 58.92 ± 0.02 (+)	- 58.66 ± 0.10	- 59.06	- 59.04	- 57.36
^{67}Ni	- 63.47 ± 0.09 - 64.07 ± 0.10 (*) - 63.741± 0.022(+)	- 63.79 ± 0.15	- 63.26	- 63.26	- 62.48
^{69}Ni		- 60.46 ± 0.15	- 60.29	- 59.86	- 59.88
^{73}Zn	- 65.41 ± 0.04 (*)	- 65.24 ± 0.15	- 65.76	- 65.21	- 65.11
^{75}Zn	-62.460± 200	- 62.70 ± 0.15	- 62.79	- 62.61	- 62.26

Mass excess in Mev, compared with the results from tables (ref. 19), from (^{14}C,^{17}O) (*) (ref. 4), from (^{4}He,^{7}Be) (ref. 14-17) (+) and with calculations.

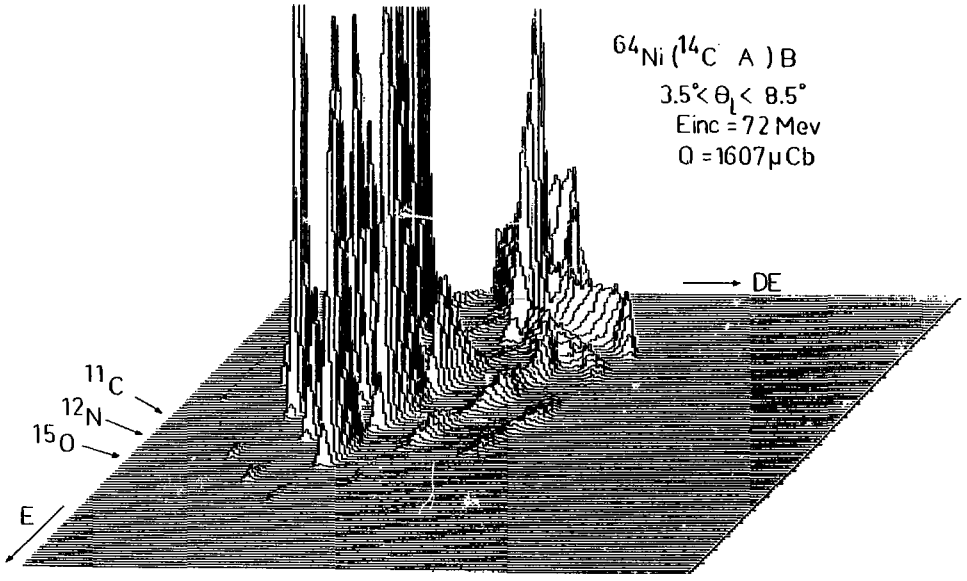

Fig. 1

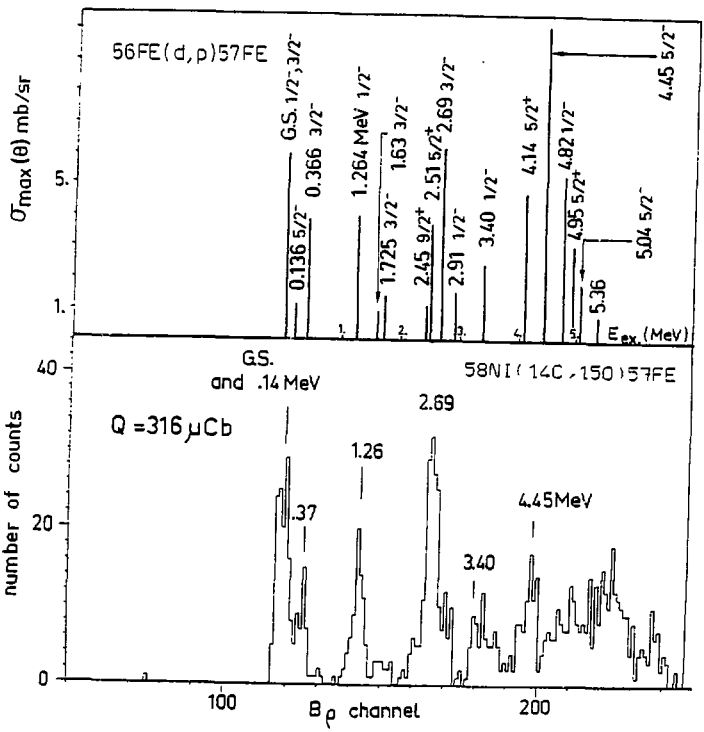
56FE(d,p)57FE
σ_{max} (θ) mb/sr
5.
1.
G.S. 1/2⁻; 3/2⁻
0.136 5/2⁻
0.366 3/2⁻
1.264 MeV 1/2⁻
1.725 3/2⁻
1.63 3/2⁻
2.45 9/2⁺
2.515/2⁺
2.69 3/2⁻
2.91 1/2⁻
3.40 1/2⁻
4.14 5/2⁺
4.95 5/2⁺
4.82 1/2⁻
5.04 5/2⁻
5.36
4.45 5/2⁻
$E_{ex.}$ (MeV)
58NI(14C,15O)57FE
G.S.
and .14 MeV
Q =316 μCb
number of counts
40
20
0
.37
1.26
2.69
3.40
4.45MeV
100
$B\rho$ channel
200

Fig. 2

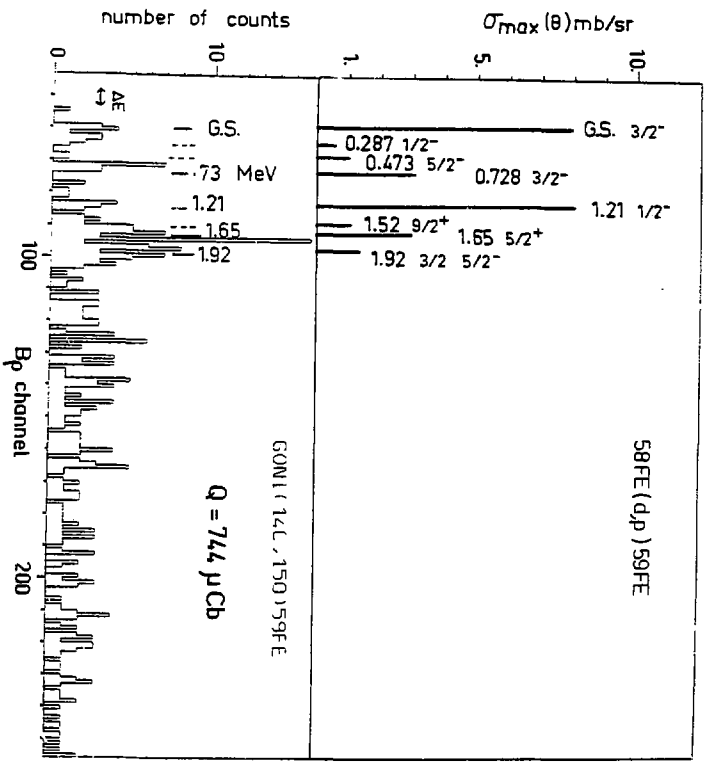
number of counts
σ_{max} (θ) mb/sr
0
10
1.
.5
.1
ΔE
G.S.
.73 MeV
1.21
1.65
1.92
100
200
Bρ channel
Q = 7.4 μ Cb
GONI (14L / 150 59FE
58FE (d,p) 59FE
G.S. 3/2⁻
0.287 1/2⁻
0.473 5/2⁻
0.728 3/2⁻
1.21 1/2⁻
1.52 9/2⁺
1.65 5/2⁺
1.92 3/2 5/2⁻

Fig. 3

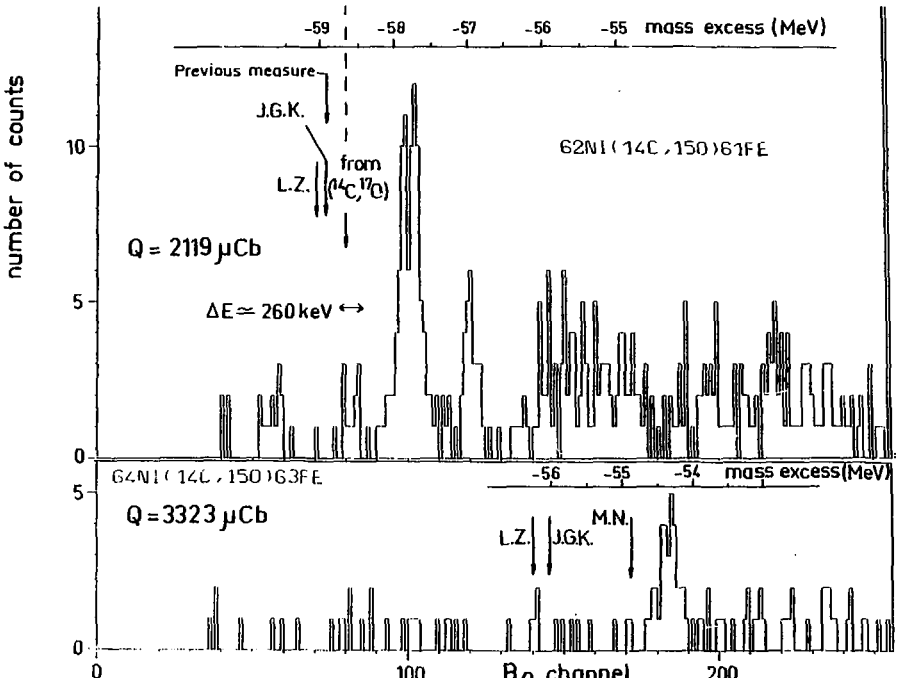
-59
-58
-57
-56
-55
mass excess (MeV)
Previous measure
J.G.K.
L.Z.
from
(14C,17O)
62Ni(14C,15O)61Fe
Q = 2119 μCb
ΔE ≃ 260 keV ↔
number of counts
10
5
0
62Ni(14C,15O)63Fe
-56
-55
-54
mass excess(MeV)
Q = 3323 μCb
M.N.
L.Z.
J.G.K.
5
0
0
100
Bρ channel
200

Fig. 4

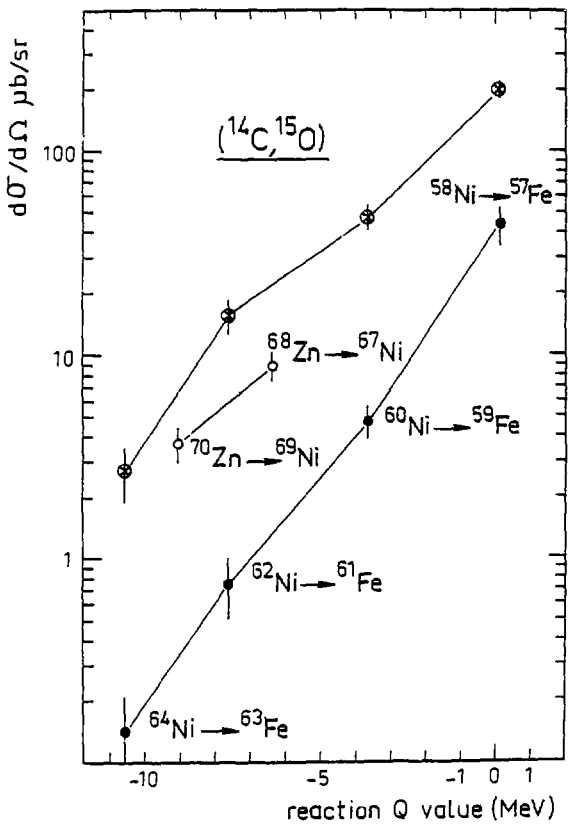
dσ/dΩ μb/sr
100
10
1
(14C,15O)
58Ni → 57Fe
68Zn → 67Ni
70Zn → 69Ni
60Ni → 59Fe
62Ni → 61Fe
64Ni → 63Fe
-10
-5
-1
0
1
reaction Q value (MeV)

Fig. 5

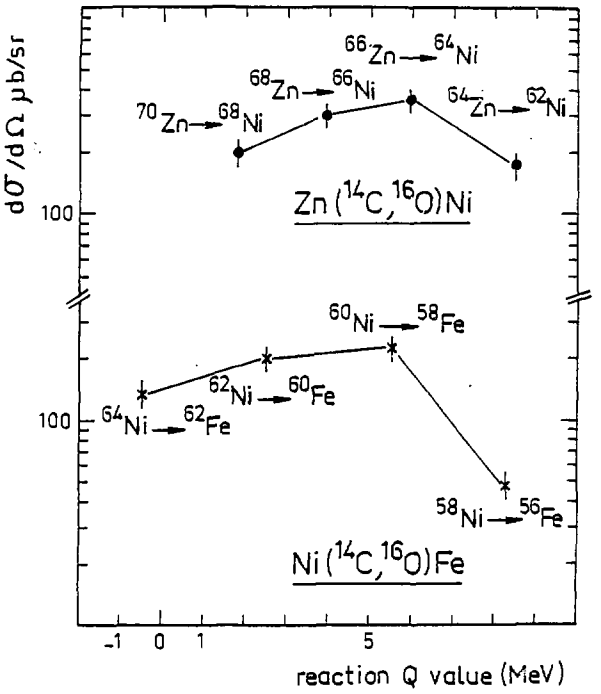
dσ/dΩ μb/sr
100
100
66Zn → 64Ni
68Zn → 66Ni
64Zn → 62Ni
70Zn → 68Ni
Zn (14C, 16O) Ni
60Ni → 58Fe
62Ni → 60Fe
64Ni → 62Fe
58Ni → 56Fe
Ni (14C, 16O) Fe
-1
0
1
5
reaction Q value (MeV)

Fig. 6a

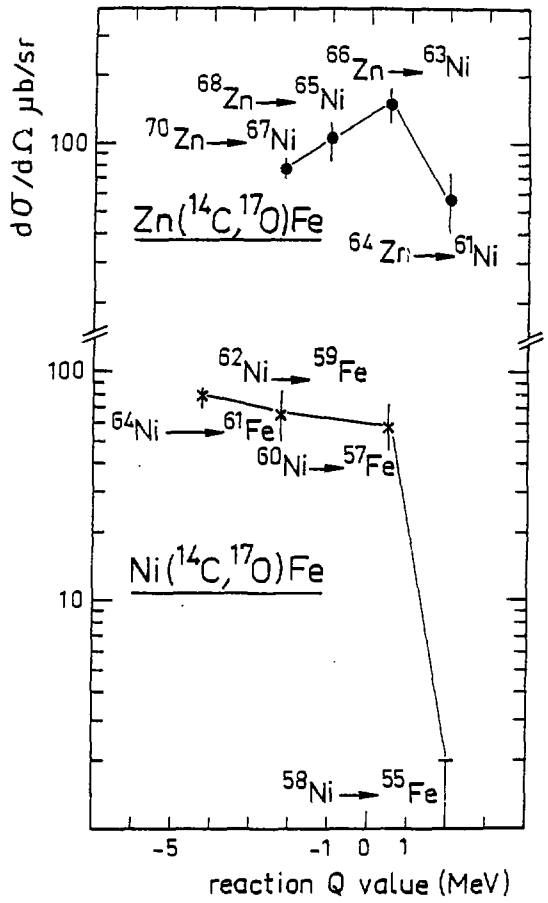
dσ/dΩ μb/sr
100
100
10
66Zn → 63Ni
68Zn → 65Ni
70Zn → 67Ni
Zn(14C,17O)Fe
64Zn → 61Ni
62Ni → 59Fe
64Ni → 61Fe
60Ni → 57Fe
Ni(14C,17O)Fe
58Ni → 55Fe
-5
-1
0
1
reaction Q value (MeV)

Fig. 6b

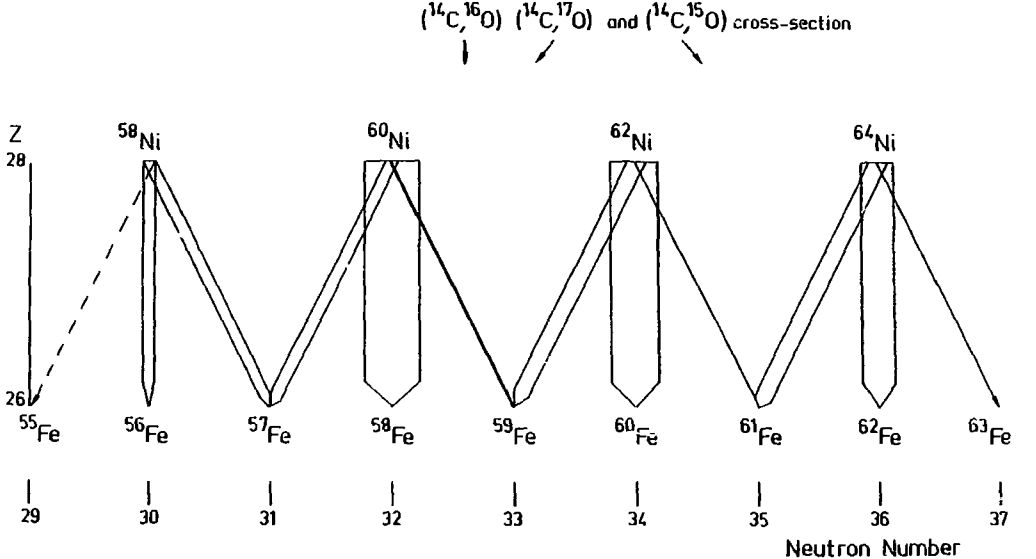
(^{14}C,^{16}O) (^{14}C,^{17}O) and (^{14}C,^{15}O) cross-section
Z
28
26
^{58}Ni
^{60}Ni
^{62}Ni
^{64}Ni
^{55}Fe
^{56}Fe
^{57}Fe
^{58}Fe
^{59}Fe
^{60}Fe
^{61}Fe
^{62}Fe
^{63}Fe
29
30
31
32
33
34
35
36
37
Neutron Number

Fig. 7

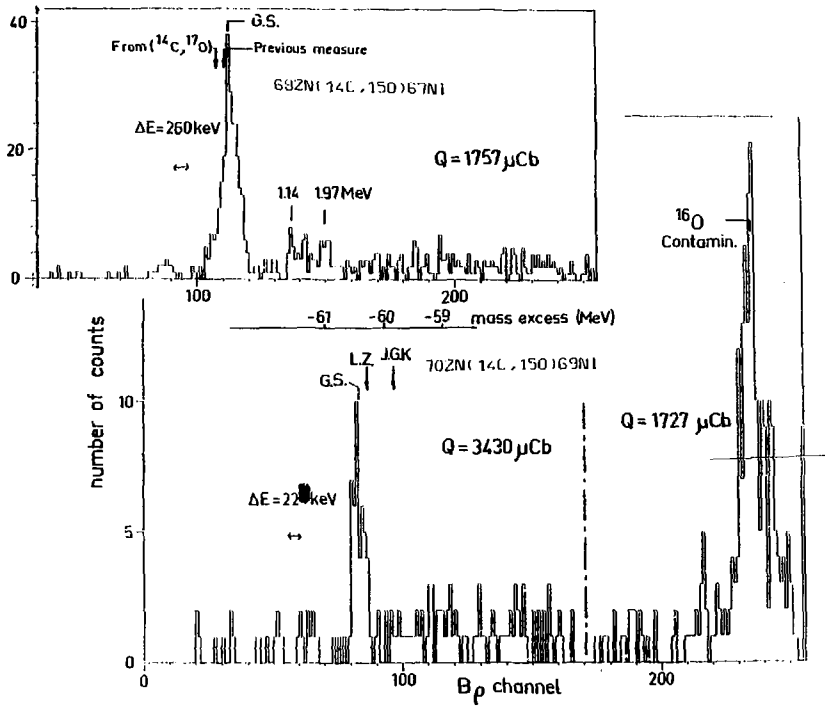
G.S.
From (^{14}C, ^{17}O)
Previous measure
68ZN(14C , 15O)67NI
ΔE=260keV
Q=1757 μCb
1.14
1.97MeV
^{16}O
Contamin.
-61
-60
-59
mass excess (MeV)
L.Z
J.G.K
70ZN(14C , 15O)69NI
G.S.
Q=3430 μCb
Q=1727 μCb
ΔE=22keV
number of counts
Bρ channel
0
100
200
40
20
10
5

Fig. 8

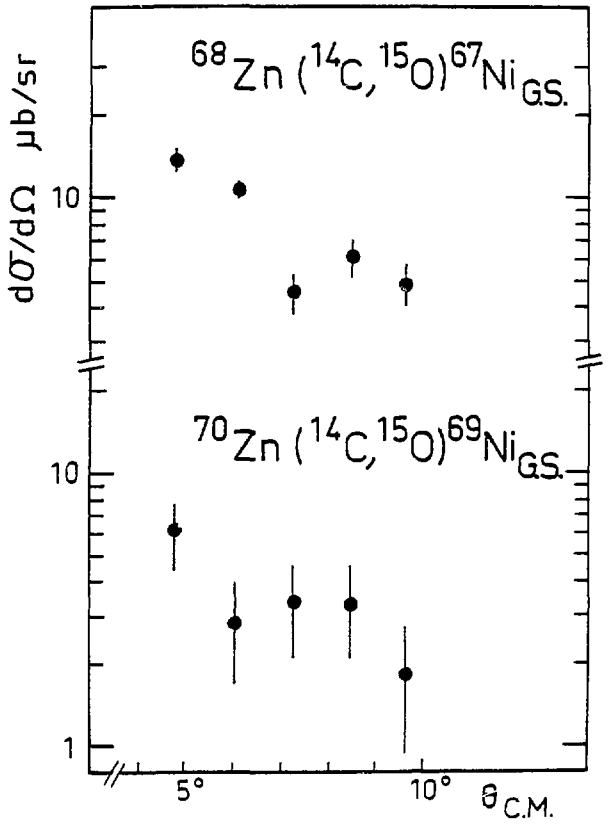
$^{68}Zn\,(^{14}C,^{15}O)^{67}Ni_{G.S.}$
$^{70}Zn\,(^{14}C,^{15}O)^{69}Ni_{G.S.}$
dσ/dΩ μb/sr
10
10
1
5°
10°
θ C.M.

Fig. 9

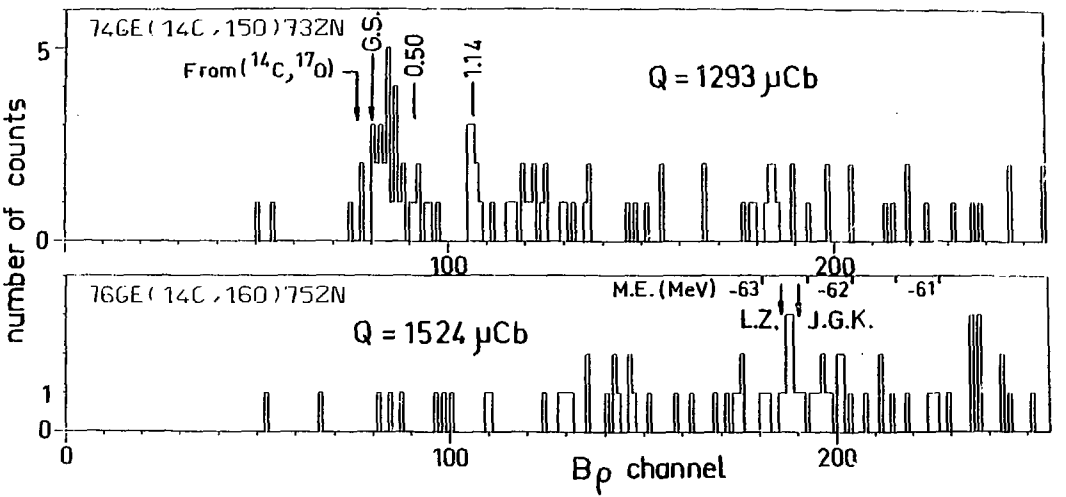
74GE(14C,15O)732N
From(14C,17O)
G.S.
0.50
1.14
Q = 1293 μCb
76GE(14C,16O)752N
Q = 1524 μCb
M.E.(MeV) -63 -62 -61
L.Z.
J.G.K.
number of counts
Bρ channel
5
0
1
100
200

Fig. 10

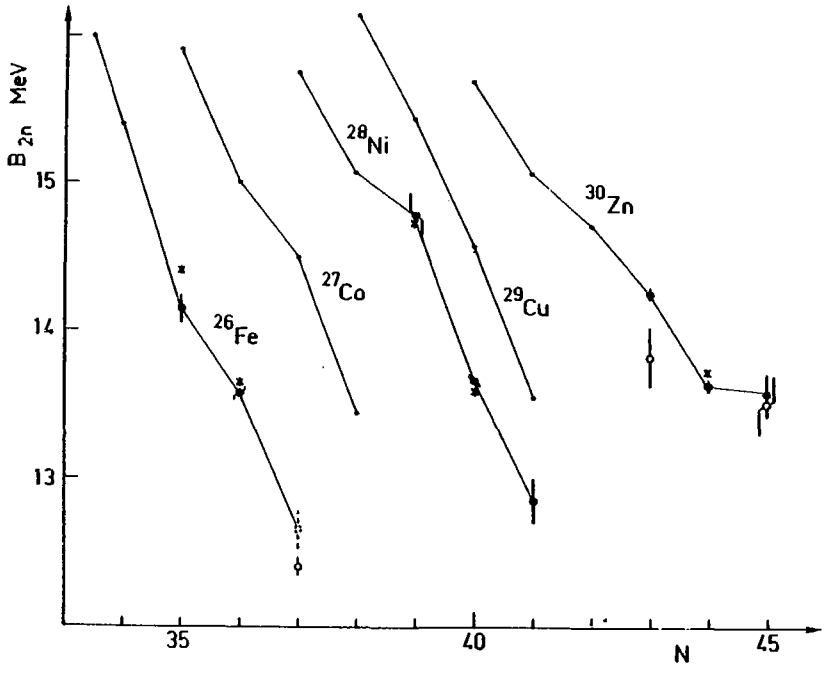

Fig. 11